Journal of Catalysis **204,** 110–117 (2001)
doi:10.1006/jcat.2001.3380, available online at http://www.idealibrary.com on IDEAL®

In Situ Solid-State Nuclear Magnetic Resonance Studies of Acetone Photocatalytic Oxidation on Titanium Oxide Surfaces

Weizong Xu and Daniel Raftery[1]

H. C. Brown Laboratory, Department of Chemistry, Purdue University, West Lafayette, Indiana 47907-1393

Received March 22, 2001; revised August 1, 2001; accepted August 1, 2001

The photocatalytic oxidation of acetone was studied on TiO_2 powder and on a TiO_2 monolayer catalyst anchored on porous Vycor glass (TiO_2/PVG) using *in situ* solid-state nuclear magnetic resonance spectroscopy. Mesityl oxide was formed by aldol condensation after acetone was adsorbed on the TiO_2 powder and its formation depended on the surface coverage of acetone. In comparison, acetone adsorption on the TiO_2/PVG surface produced a chemisorbed propylene oxide surface species. Propylene oxide was strongly adsorbed on the TiO_2/PVG surface and resistant to evacuation, while mesityl oxide was relatively weakly adsorbed on the surface and could be pumped away. No propylene oxide species was observed on the TiO_2 powder. The photooxidation of acetone proceeded through two routes: The first was through the fragmentation of mesityl oxide to formic acid, which formed titanium formate and a surface OH group. Formate was further oxidized to the final oxidation product CO_2. This process proceeded at a very slow rate. As a result, the oxidation rate of acetone was very slow on the TiO_2 powder catalyst at high (greater than one monolayer) coverage. The second route was through the oxidation of the chemisorbed propylene oxide species, which was oxidized to acetic acid and then to CO_2 at a much faster rate. The faster conversion rate of acetone observed on TiO_2/PVG was due to the availability of this oxidation route.

1. INTRODUCTION

The widespread use of volatile organic compounds (VOC) in both domestic applications and industrial processes has caused significant environmental problems. Approximately 50% of the priority pollutants on the U.S. Environmental Protection Agency's (EPA) list are composed of VOCs (1). Therefore, a great deal of attention has been paid by scientists in recent years towards the development of measures to convert these pollutants into nontoxic compounds such as CO_2 and H_2O. Among these detoxification measures, the use of semiconductor photocatalysts such as TiO_2, ZnO, MgO, and CdS represents a promising technology due to a number of favorable factors. Three such factors are (i) photocatalytic oxidation (PCO) can proceed at ambient temperature and pressure; (ii) the excitation source can be sunlight or low-cost fluorescent light sources; and (iii) semiconductor photocatalysts are generally nontoxic, inexpensive, and chemically and physically stable. A number of researchers have reviewed the important features and summarized the research progress regarding semiconductor photocatalysis at both liquid–solid and gas–solid interfaces (2–4). A number of factors contribute to the complexity of PCO processes: the identity, phase, and concentration of pollutants; the morphology and structure of semiconductor catalysts; the type and intensity of light source; the presence of surface-adsorbed water; and the oxygen concentration. A complete description of the photocatalytic mechanisms is still lacking, and thus a number of detailed studies will be required to improve our understanding of this promising technology.

Aldehydes, ketones, and alcohols have been regarded as the central class of VOCs responsible for poor air quality since these compounds comprise the most widely used organic solvents (5–8). In addition, acetone is a major intermediate for 2-propanol PCO and therefore an understanding of its oxidation is important for the PCO of alcohols. As detailed in the following, we report solid-state nuclear magnetic resonance (SSNMR) studies on the PCO of acetone, a model ketone compound. The major objectives of this investigation are to understand the role of intermediates in determining the acetone PCO rate and ultimately to increase the photoefficiency of its degradation. As early as 1971, Munuera and Stone (9) studied the adsorption behavior of acetone on rutile TiO_2. Using adsorption isotherms and temperature-programmed desorption (TPD), they found chemisorption sites for both 2-propanol and acetone and that 2-propanol has a stronger interaction with the TiO_2 surface than acetone. Falconer and co-workers (10) also found chemisorption sites of acetone on the TiO_2 surface using TPD and temperature-programmed oxidation (TPO) methods. In addition, they found that molecularly adsorbed acetone desorbed more easily than the acetone formed as an intermediate during 2-propanol PCO. Most groups found that acetone was

[1] To whom correspondence should be addressed. E-mail: raftery@purdue.edu.

0021-9517/01 $35.00

cleanly converted to final products, i.e., CO_2 and water, after its PCO (5, 6, 8, 10, 11), although Bickley and coworkers reported that trace amounts of formic acid and acetaldehyde were produced (12, 13). The format of intermediate species and/or possible partial oxidation products on the surface could be justified according to the mass balance, although no partial oxidation products were observed in the gas phase. For example, no partial oxidation products were detected at low conversions (0.7–9.6%) of acetone (5, 8) in the outlet stream using gas chromatography (GC) analysis equipped with a flame ionization detector, indicating that they were mineralized on the surface. Recently, El-Maazawi *et al.* (14) reported their observation that surface-bound mesityl oxide results from the aldol condensation of acetone upon its adsorption on TiO_2 powder. The quantity of formed mesityl oxide and the photooxidation behavior of acetone depended on the acetone surface coverage. We have recently observed mesityl oxide formation during the 2-propanol photooxidation on TiO_2 as well, where acetone is a major intermediate species (15).

The majority of PCO studies to date have been carried out under steady-state conditions, and therefore the mechanistic information has been inferred from observed gas-phase intermediates and products and the rate dependence on their concentrations. In the case of acetone PCO, the formation of chemisorbed acetone species and the presence of partial oxidation products and/or intermediates have been inferred, but the identity of these surface species is still elusive. To explore the reaction mechanisms in heterogeneous photocatalysis, precise identification of the reaction intermediates and *in situ* monitoring of the evolution of surface species during PCO are important. We (15–21) and others (22, 23) have shown that SSNMR can provide invaluable and complementary structural and dynamic information for a variety of PCO reactions due to NMR's atomic specificity, high resolution, and quantitative capabilities. In particular, SSNMR is well suited for following the formation and evolution of surface-bound species on the catalysts. In this work, we report *in situ* observations of the evolution of surface species during acetone PCO, which provide insight into the reaction mechanisms at the gas–solid interface.

In addition to improving our knowledge about photocatalytic mechanisms, another important driving force is enhancement of the oxidation efficiency. It is well known that acetone PCO occurs at a very slow rate. Therefore, a number of research groups have made an effort to improve external conditions such as light intensity, reaction temperature, water content, and acetone coverage (7, 8, 10, 14, 24, 25), while others have pursued improvements through modification of the catalyst itself. Generally, a thin film of catalyst particles is physically coated onto a support such as alumina foam (26), paper (27), fiberglass cloth (11), fused-silica glass fibers (8), optical microfibers (18, 20), tungsten mesh (28–31), or ceramic honeycomb monoliths (7, 25). Much attention has also been paid to the chemical modification of support materials by anchoring one or more monolayers of TiO_2. This has been done by the reaction of $TiCl_4$ with surface OH groups of porous Vycor glass (32–36) or recently by metal ion implantation (37). One advantage of chemical modification is that the surface coverage or content of the photocatalyst can be controlled completely through a synthetic procedure. Furthermore, it has been demonstrated that the photocatalytic activity of the supported monolayer catalyst was higher than that of the TiO_2 powder for some reactions such as the reaction of C_3H_4 with water (32), the reduction of CO_2 (38) and degradation of (liquid-phase) 1-octanol (34) on TiO_2/PVG, and the gas-phase PCO of acetone on metal ion implanted $Ti_{1-x}V_xO_2$ (37). In this paper, we compare the acetone PCO behavior on TiO_2 powder and a TiO_2 monolayer catalyst anchored on porous Vycor glass (TiO_2/PVG). SSNMR studies provide insight into several of the factors that influence the photocatalytic behavior. A possible mechanism for acetone PCO will also be proposed.

2. EXPERIMENTAL

2.1. Catalyst Preparation

Photocatalytic oxidation reactions were performed under batch conditions at room temperature using samples that were sealed in glass NMR tubes. Our procedures for preparing catalyst samples of TiO_2 powder and TiO_2/PVG have been described in detail elsewhere (15–21).

TiO_2 powder catalyst. Briefly, about 170 mg of TiO_2 powder (Degussa P-25, approximately 70% anatase and 30% rutile; BET surface area 55 $m^2\ g^{-1}$) was packed into a 5-mm glass NMR tube (Norell), which was then attached to a gas manifold. The powder was first evacuated at 773 K in a ceramic heater for 4 h to remove the adsorbed species and then calcined at 773 K for another 4 h under 1 atm of O_2. The powder was then evacuated to 5×10^{-5} Torr, and allowed to cool to room temperature in preparation for loading acetone.

TiO_2/PVG catalyst. A monolayer TiO_2/PVG catalyst was prepared using the hydrolysis of gas-phase $TiCl_4$ with OH groups on the PVG surface (32–34). A 3.6-mm-diameter PVG rod (Corning 7930, BET surface area $\sim$150 m^2/g, pore diameter 40 Å) was fitted into a 5-mm glass NMR tube (Norell). The PVG rod weighed about 170 mg and was 12 mm in length. The glass NMR tube was then attached to a gas manifold and the PVG rod was degassed and calcined for 4 h. To ensure the formation of a saturated TiO_2 monolayer coverage, the calcined PVG rod underwent a series of four reaction cycles with 88 μmol of $TiCl_4$ (Aldrich), which was introduced by gas-phase adsorption. The HCl produced by the reaction

of $TiCl_4$ with the surface OH groups was then evacuated after each cycle. Due to the dry reaction conditions, the formation of multiple monolayers was excluded. Once the $TiCl_4$ was anchored on the PVG, the catalyst was hydrated, degassed, and calcined for 4 h under 1 atm of O_2 at 773 K. The TiO_2/PVG catalyst was then evacuated to 5×10^{-5} Torr, and allowed to cool to room temperature before loading with reagents. We have previously prepared one, two, three and four monolayers of TiO_2 on PVG and measured their UV and X-ray diffraction (XRD) spectra. The UV spectrum of the monolayer TiO_2/PVG catalyst indicated that its band gap is larger than that of the TiO_2 powder, and the band gap decreases and approaches that of the TiO_2 powder as the number of TiO_2 monolayers is increased (21, 32). In addition, according to XRD data, the structure of the TiO_2 surface layer(s) is similar to the structure of anatase at three- and four-monolayer coverages (21).

2.2. Sample Preparation

Uniformly labeled acetone ($^{13}CH_3^{13}CO^{13}CH_3$, Cambridge Isotope) was loaded onto the previously calcined catalysts at room temperature using a gas manifold. Three amounts of acetone (48, 96, or 192 μmol) along with 90 μmol of O_2 were loaded onto TiO_2 powder catalysts. To evaluate the surface coverage, a BET analysis of acetone adsorbed on the TiO_2 powder was performed. A one-monolayer coverage of acetone was found to correspond to 5.0 molecules/ nm^2 on the TiO_2 (Degussa P25) powder, a value which is between two previously reported coverages of 3.0 and 10.0 molecules /nm^2 (7, 14). The reported saturation coverage (3.0 molecules/nm^2) of acetone on the Degussa powder was measured by TPD and TPO in an annular reactor. As the authors pointed out (7), the reported saturation coverage could be low since (i) some acetone was weakly adsorbed and slowly desorbed at room temperature before the TPD/TPO experiment and (ii) a significant amount of decomposed products remained on the surface and therefore were not detected. According to our BET data, a one-monolayer coverage of acetone corresponds to 82 μmol for 170 mg of Degussa TiO_2 powder. A calibration curve of the gas-phase pressure versus the total acetone loading was also made to evaluate the percentage of gas-phase acetone at each sample loading. Since the dead volume of the NMR tube is very small ($\sim$ 0.3 ml), the amount of acetone in the gas phase is limited to a maximum of 3.7 μmol at its saturated vapor pressure, 231 Torr at 298 K. Therefore the gas-phase content is limited to less than 2% of the total acetone in each sample. The sample loadings, evaluation of the gas-phase percentages, and surface coverages for each of the three TiO_2 powder samples (SI–SIII) are listed in Table 1.

A fourth sample (SIV) was prepared by loading 32 μmol of acetone and 90 μmol of O_2 on the TiO_2/PVG catalyst, which corresponds to a 1/5 monolayer coverage on the PVG surface. The coverage calculation is based on the surface area of PVG (150 m^2/g). A sample of acetone adsorbed on pure PVG with the same loading (32 μmol) was also prepared as a control experiment. After samples were loaded, all glass NMR tubes were flame sealed 10–12 mm above the catalyst sample.

TABLE 1

Acetone Coverages on the TiO_2 Powder and TiO_2/PVG Photocatalysts

Sample	Total loading (μmol)	Surface coverage (monolayer)	Gas phase (%)
SI	48	0.58	0.6
SII	96	1.2	1.0
SIII	192	2.3	1.2
SIV(PVG)	32	0.2	—

2.3. In Situ SSNMR Methods

A home-built magic angle spinning (MAS) probe and light delivery system were used for *in situ* photocatalytic studies (17). A 300-W Xe-Arc lamp (ILC) was used as the UV source. Light in the wavelength range of 350 to 450 nm was selected using a dichroic mirror (Oriel Corp.). The near-UV light was delivered to the sample located inside the NMR magnet using a liquid-filled optical light guide (Oriel Corp.). The MAS probe was doubly tuned for ^1H and ^{13}C observation at frequencies of 300 and 75.4 MHz, respectively, and was capable of spinning the sealed samples up to 2.7 kHz. The near-UV light irradiating on the NMR sample has been previously measured to be 5 mW. To increase the light intensity irradiating the sample, *ex situ* irradiation was also utilized.

3. RESULTS AND DISCUSSION

3.1. Adsorption of Acetone on Catalyst Surfaces

The adsorption of acetone on the TiO_2 powder and TiO_2/PVG catalysts was examined using proton-decoupled ^{13}C-MAS Bloch Decay (BD) and ^{13}C-CP/MAS NMR spectra. By combining BD and CP/MAS spectra, the relative mobility of different species can be evaluated and the surface species can be identified. The signal intensity of the CP/MAS spectrum is closely related to the mobility of the surface-adsorbed species. Although CP/MAS spectra can be somewhat nonquantitative, in conjunction with quantitative BD, CP/MAS NMR can be a very useful assignment tool for surface analysis.

TiO_2 powder catalyst. The proton-decoupled ^{13}C-BD and corresponding CP/MAS NMR spectra of TiO_2 powder samples SI, SII, and SIII before irradiation are shown in

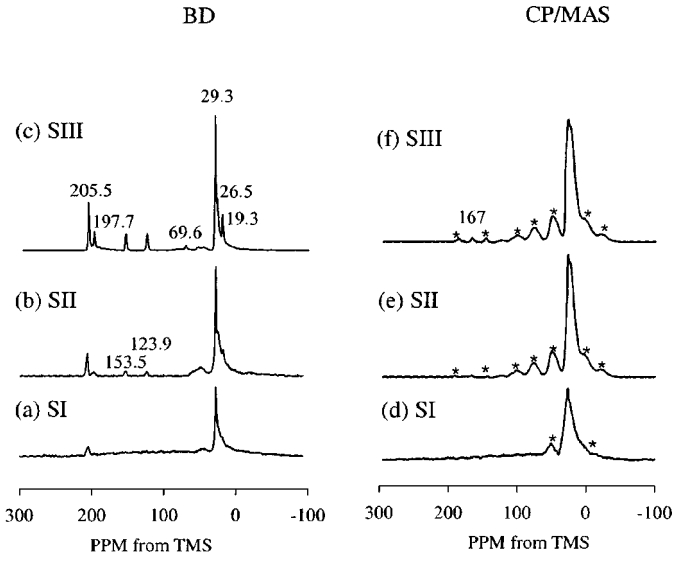

FIG. 1. Proton-decoupled ^{13}C-MAS BD and corresponding proton-decoupled ^{13}C-CP/MAS spectra at different acetone surface coverages on TiO_2 powder. BD (a) sample SI (0.58 monolayer coverage), (b) SII (1.2 monolayers), (c) SIII (2.3 monolayers). CP/MAS (d) SI, (e) SII, (f) SIII. Each spectrum consists of the average of 200 transients with a recycle delay time of 10 s. The CP/MAS spectra were obtained using a 50-μs contact time and 2.0-kHz spinning speed. Asterisks indicate spinning sidebands of surface bound species.

Fig. 1. In addition to the physisorbed acetone species, it has been shown that the adsorption of acetone on the metal oxide surface can yield different products through aldol condensation and secondary reactions such as double-bond migration, hydride transfer, and cracking (39, 40). The extent of the reaction and the selectivity for various products depend on the surface acidity of metal oxides and the reaction conditions. El-Maazawi *et al*. (14) recently reported their observation of acetone aldol condensation on TiO_2 using FTIR methods. In a previous study of 2-propanol PCO (15), we also observed acetone aldol condensation because of the fact that acetone is the main intermediate formed during 2-propanol PCO. In the BD spectra, the physisorbed acetone appears at 205.5 and 29.3 ppm in three samples, which are close to the chemical shifts (206.6 and 30.8 ppm) for acetone dissolved in liquid-phase $CDCl_3$ (41). The narrow linewidth of these peaks indicates that the acetone is weakly bound to the surface. Weakly surface-bound acetone exchanges rapidly between the surface and the gas phase since no unique resonance is observed for the gas-phase species. In addition to adsorbed species, in our sealed samples a small amount of gas-phase acetone is present as well, and its percentage in each sample is listed in Table 1. As the surface coverage increases, several additional peaks become distinguishable and their intensity increases with the surface coverage. The weak peaks at 69.6 and 54.0 ppm observed in sample SIII are assigned to 4-hydroxyl-4-methyl-2-pentanone (diacetone alcohol), the first product of acetone aldol condensation (39). The peaks at 19.3, 26.5, 123.9, 153.5, and 197.5 ppm can be ascribed to the mesityl oxide species, the further dehydration product of diacetone alcohol on the TiO_2 surface. The quantity of mesityl oxide formed increases as a function of acetone surface coverage on TiO_2, in accordance with the observation of El-Maazawi *et al*. (14). All these peaks correspond well to the liquid-phase peaks for mesityl oxide dissolved in $CDCl_3$ (41). Table 2 lists the chemical shifts of different surface species found in this study and their corresponding liquid-phase values.

To examine species with restricted mobility, CP/MAS spectra were collected using a short CP contact time of 50 μs. As shown in Figs. 1d–f, the species at 29.0 ppm is relatively strongly adsorbed on the surface as indicated by the presence of spinning sidebands. This species can be assigned to acetone, which is bound to the surface via hydrogen bonding. Since the carbonyl carbon has no attached hydrogen, its cross-polarization efficiency is very limited and hence no corresponding signal was observed at 205 ppm in the CP/MAS spectra. In addition, the peaks corresponding to the mesityl oxide are not observed in the CP spectrum, indicating that the mesityl oxide is relatively weakly adsorbed on the surface. A new peak with several sidebands is also found at 167 ppm in the CP/MAS spectrum of sample SII and becomes more visible as the acetone surface coverage increases. This peak corresponds to formate (42, 43) which is strongly bound to the TiO_2 surface. FTIR spectra of adsorbed acetone on TiO_2 confirm the presence of formate species (44). A characteristic peak at 1575 cm^{-1} (ν_{as}(COOTi)) (14) corresponding to titanium formate appears after acetone is adsorbed on TiO_2 and becomes more intense as the UV irradiation proceeds. This

TABLE 2

^{13}C Chemical Shifts of Different Species on TiO_2 Powder and TiO_2/PVG

Catalyst	Species	Chemical shift (ppm)
TiO_2 powder	Acetone	205.5; 29.3
	Diacetone alcohol	69.6; 54.7
	Mesityl oxide	19.3; 26.6; 123.9; 153.5; 197.7
	Titanium formate	167
	CO_2	124
TiO_2/PVG	Acetone	215.0; 28.0
	Mesityl oxide	22; 205
	Propylene oxide	50
	Acetic acid	18.8; 170
	CO_2	124
	CO	183
Liquid acetone in $CDCl_3$		30.8; 206.6 (41)
Liquid mesityl oxide in $CDCl_3$		20.55; 27.48; 124.30; 154.56; 198.23 (41)
Liquid propylene oxide in $CDCl_3$		48.22; 48.00; 18.03 (41)

species most likely results from the thermal fragmentation of mesityl oxide to formic acid, followed by a dehydrogenation reaction of formic acid with the surface. This species was only observed at a high acetone surface coverage.

PVG/TiO_2 catalyst. The proton-decoupled ^{13}C-BD and corresponding ^{13}C-CP/MAS spectra of acetone adsorbed on TiO_2/PVG (sample SIV) are shown in Fig. 2. The two intense and narrow peaks at 28.0 and 215.0 ppm correspond to molecularly adsorbed acetone. The weak, broad peaks at 22 and 205 ppm are assigned to a small amount of mesityl oxide that forms, while the other mesityl oxide resonances are too weak to be observed in this sample. No formate peak was found here, as expected, due to the low surface coverage of acetone used in this sample. Note that the chemical shift of carbonyl acetone on PVG/TiO_2 (215 ppm) is very different from that on Degussa TiO_2 powder (205.5 ppm). The chemical shift of the carbonyl carbon in acetone is known to be very sensitive to the interaction of the carbonyl oxygen with surface acid sites. This property makes acetone a sensitive probe of surface acidity. In fact, the ^{13}C-chemical shift in acetone can vary from 206 ppm in $CDCl_3$ to 250 ppm at superacid sites (45, 46). The larger chemical shift of acetone observed on the TiO_2/PVG surface suggests that its OH groups are more acidic than those on the TiO_2 powder surface. Similar results using ammonia as a surface probe have also been reported for TiO_2/SiO_2, which has much stronger acid sites than either TiO_2 or SiO_2 oxides (47).

An additional broad peak at 50 ppm was observed in the BD spectrum (Fig. 2a), and was also observed in the CP/MAS spectrum at two different spinning speeds of 1.4 and 2.0 kHz (Fig. 2b) using a 50-μs contact time. This unusual peak corresponds to a new surface species. Note that this peak was not found in the sample of acetone adsorbed on TiO_2 powder nor during 2-propanol PCO on TiO_2/PVG (15), where acetone is a major intermediate. In addition, a sample was made using the same loading of acetone and O_2 on a pure, calcined PVG sample and the spectrum showed only the physisorbed acetone peaks at 28.0 and 215 ppm (not shown). No aldol condensation product nor peak at 50 ppm were observed. These results indicate that the formation of the species appearing at 50 ppm is unique to the surface of TiO_2/PVG. We identify this peak as a strongly bound propylene oxide species for the following reasons. First, the chemical shifts of $^{13}CH_2$ and ^{13}CH in propylene oxide occur at very close values (48.22 and 48.00 ppm in $CDCl_3$) (41) and match our observed chemical shift on the surface quite closely. Second, the structural similarity between propylene oxide and 2-propoxide suggests a higher PCO activity of propylene oxide, as has been observed for the high reactivity of the 2-propoxide species (10, 15). We will discuss the PCO of propylene oxide further in the following section. Finally, the fact that the observed peak is only evident in the CP/MAS spectrum suggests the formation of a bond between the propylene oxide and the TiO_2 surface, which is very possibly strong hydrogen bonding with a surface OH group. We also note that the formation of the propylene oxide species is unique to the TiO_2/PVG catalyst. A TiO_2 powder sample with the same low acetone coverage (0.2 monolayers) did not show the formation of propylene oxide. Therefore, its formation appears to be related to either the difference in the surface morphology or the acidity of the TiO_2/PVG catalyst.

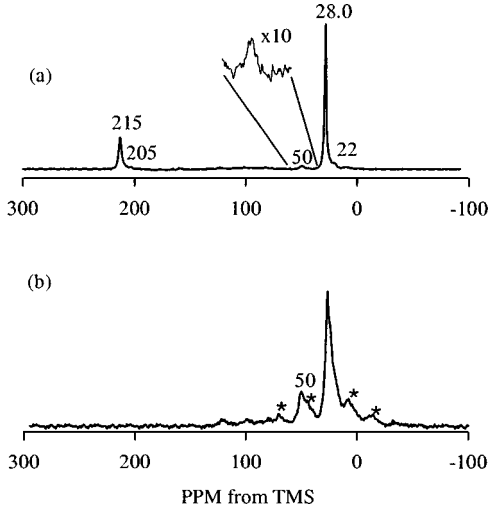

FIG. 2. Proton-decoupled ^{13}C-MAS BD (a) and corresponding CP/MAS at 2.0 kHz spinning speed. (b) NMR spectra of acetone on TiO_2/PVG (sample SIV).

3.2. *Photocatalytic Oxidation of Acetone*

TiO_2 powder catalyst. The photocatalytic oxidation of acetone on TiO_2 powder was observed to be very slow. No oxidation products, e.g., CO_2, were found even after 5 h of *ex situ* irradiation (using approximately 100 times greater irradiation intensity) for samples SI and SII. However, the intensity of the peaks corresponding to mesityl oxide was observed to change slightly in the BD spectra. After 10 h of *ex situ* irradiation, sample SII showed a small quantity of CO_2 formation in the BD spectrum and a slightly more intense formate peak at 167 ppm in the CP/MAS spectrum (Fig. 3). Formate is strongly adsorbed on the TiO_2 surface, as is indicated by the observed sidebands. As a result, it will not desorb from the surface unless it is further oxidized to CO_2. This explains why many of the previous studies that focused on the determination of gas-phase species observed the clean oxidation of acetone only. Therefore, the oxidation route of acetone on TiO_2 powder in our study is observed through mesityl oxide fragmentation to formic acid, which forms titanium formate with a surface OH group and then the final oxidation product CO_2. This process proceeds at a very slow rate. The proposed mechanism for acetone PCO on TiO_2 powder is shown in Fig. 4. In order to enhance the PCO rate of acetone on TiO_2 powder, it is possible to raise

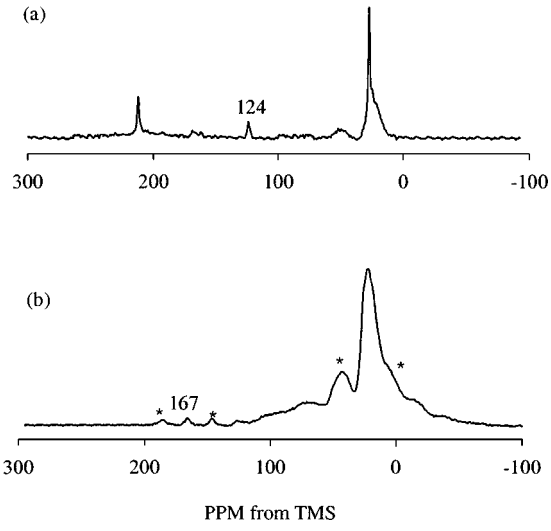

FIG. 3. Proton-decoupled ^{13}C-MAS BD (a) and CP/MAS (b) spectra of acetone sample SII on TiO_2 powder after 10 h of *ex situ* irradiation.

the oxygen concentration (10). We have also conducted several of these experiments at higher O_2 concentrations using FTIR detection methods and found that the acetone PCO could proceed much faster than in the present case where the O_2/acetone ratio is at most 2 : 1. A detailed report of these findings as well as studies on the nature of the irradiation and kinetics will be made in a separate publication (44). Another possible method to enhance the PCO rate is to decrease the acetone coverage, as El-Maazawi *et al.* (14) have reported.

TiO_2/PVG catalyst. Photocatalytic oxidation of acetone on TiO_2/PVG was examined as a function of the irradiation time, and these results are shown in Fig. 5 for the BD spectra and Fig. 6 for the CP/MAS spectra. As the BD spectra indicate, CO_2 was produced in the first 2 h of *in situ* irradiation. This indicated that the PCO rate of acetone on TiO_2/PVG is much higher than that on TiO_2 powder. In additional, *ex situ* irradiation was also carried out. New peaks

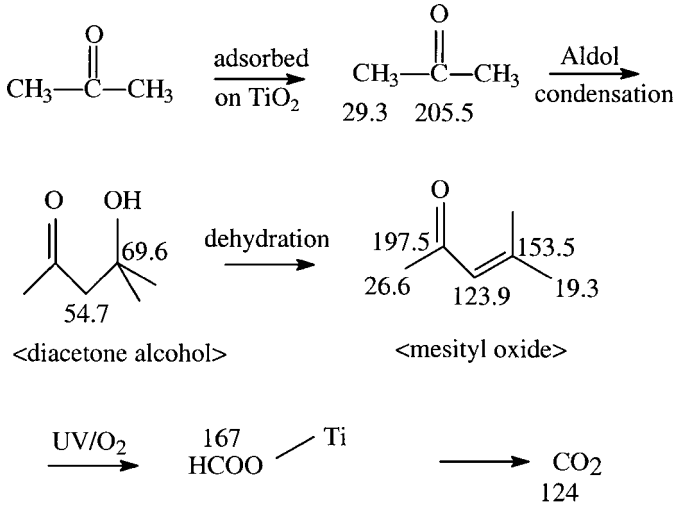

FIG. 4. Proposed mechanism for acetone photooxidation on TiO_2 powder.

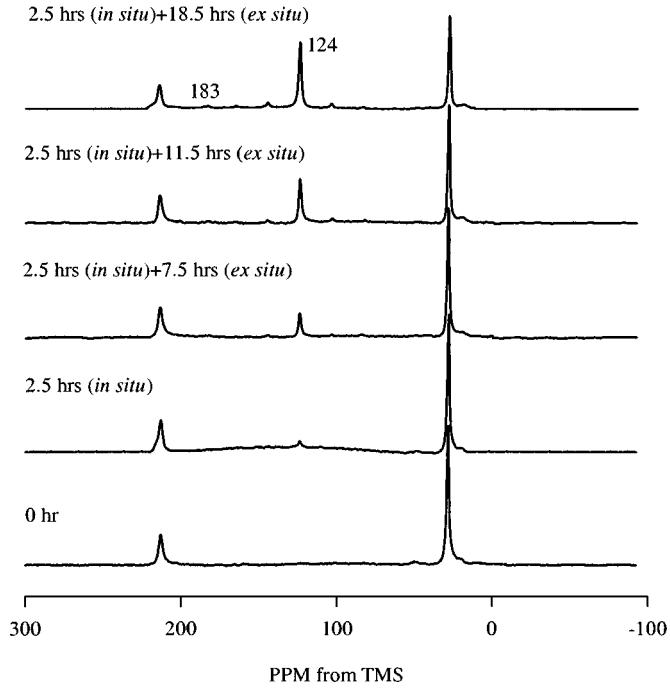

FIG. 5. Proton-decoupled ^{13}C-MAS BD spectra of acetone on TiO_2/PVG during photocatalytic oxidation. Irradiation times are indicated.

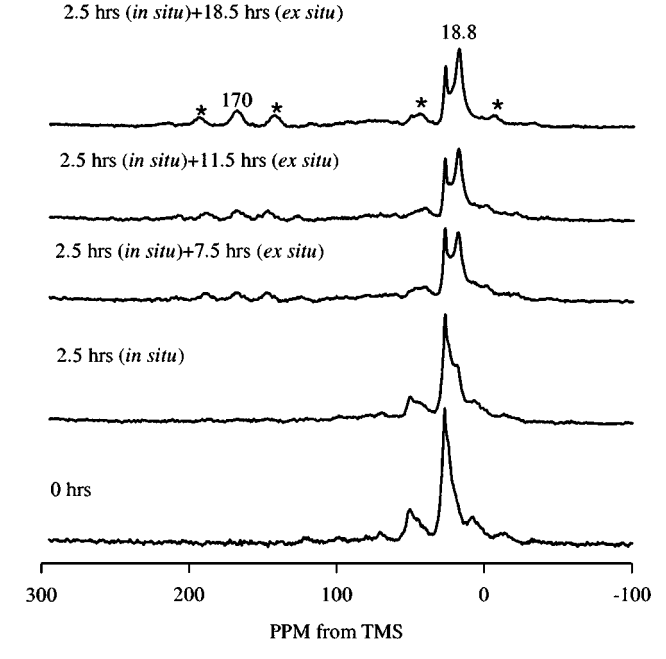

FIG. 6. Proton-decoupled ^{13}C-CP/MAS spectra of acetone on TiO_2/PVG during photocatalytic oxidation. Irradiation times are indicated.

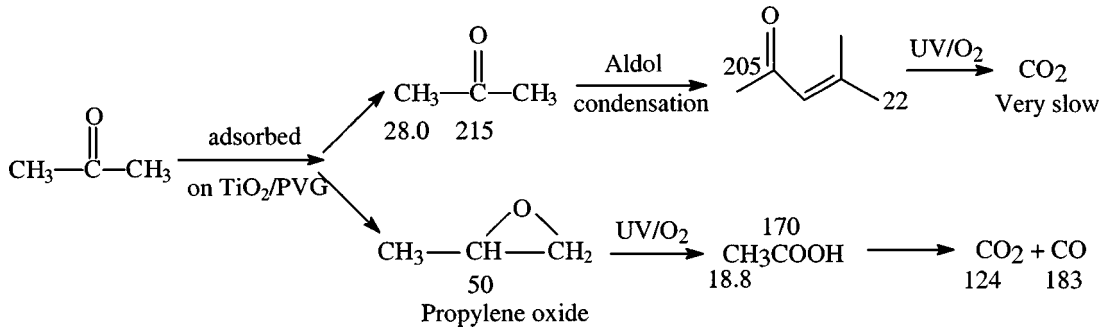

FIG. 7. Proposed mechanism for acetone photooxidation on TiO_2/ PVG.

at 18.8 and 170 ppm appeared in the CP/MAS spectra, accompanied by a decrease in intensity of the propylene oxide peak at 50 ppm during UV irradiation. However, the propylene oxide peak at 50 ppm was not completely consumed even after a long *ex situ* irradiation period. This indicated that an equilibrium was established among the acetone reactant, propylene oxide, which is a strongly adsorbed surface species, and acetic acid, which has peaks at 18.8 and 170 ppm. Acetic acid is also strongly adsorbed on the surface, as evidenced by the presence of spinning sidebands. After long period of *ex situ* irradiation, CO (183 ppm) was also found. Notice that the CO_2 peak was found to have some weak spinning sidebands, indicating that a small fraction of CO_2 was strongly bound to the surface.

To determine whether the faster PCO of acetone on TiO_2/PVG is exclusively due to the presence of the propylene oxide surface species, an acetone sample with the same loading as that in sample SIV was loaded and then subjected to evacuation to a pressure of 10^{-5} Torr. The collected CP/MAS and BD spectra (not shown) indicate that the propylene oxide surface species was not affected by evacuation, whereas an obvious decrease of the peak intensity corresponding to physisorbed acetone and mesityl oxide was observed. The PCO behavior on this evacuated sample, including acetic acid and CO_2 formation, showed trends very similar to those of the nonevacuated sample (sample IV).

In comparison to the slow oxidation of acetone on the TiO_2 powder, we can conclude that fast oxidation of acetone on TiO_2/PVG is mainly due to the formation of propylene oxide and its conversion to acetic acid and CO_2, whereas the slow mesityl oxide fragmentation was negligible. The proposed mechanism for acetone on TiO_2/PVG is shown in Fig. 7.

4. CONCLUSIONS

The photocatalytic oxidation of acetone on TiO_2 powder and TiO_2/PVG has been investigated using *in situ* SSNMR methods. The following conclusions can be derived from this work.

1. Acetone adsorbs on TiO_2 powder to form a physisorbed, H-bonded species. Aldol condensation of acetone was also observed, forming diacetone alcohol followed by dehydration to yield mesityl oxide. As the acetone surface coverage increases, the aldol condensation becomes more favorable and more mesityl oxide is formed.

2. A new chemisorbed propylene oxide surface species was identified after acetone was adsorbed on the TiO_2/PVG surface. Propylene oxide was resistant to evacuation. Mesityl oxide, which was also observed on the TiO_2/PVG surface after adsorption of acetone, is only weakly adsorbed on the surface and hence can be pumped away after evacuation.

3. The photooxidation of acetone can proceed through two routes: One is through the fragmentation of mesityl oxide to formic acid, which forms titanium-bound formate and a surface OH group. Formate is further oxidized to CO_2. This process is found at high acetone coverages on TiO_2 powder, and proceeds at a very slow rate. The second route is through the oxidation of a chemisorbed propylene oxide species, which is only found on TiO_2/PVG and not on Degussa P-25 TiO_2 powder catalysts. Propylene oxide is oxidized to acetic acid and then to CO_2 at a much faster rate.

4. The photooxidation behavior of the TiO_2 catalysts studied here depends significantly on surface morphology, because of the possibility of forming different chemisorbed species. This point can be illustrated by comparing the PCO behavior of acetone to that of 2-propanol (15). The formation of propylene oxide after acetone is adsorbed on TiO_2/PVG allows acetone oxidation to proceed much faster than on the TiO_2 powder catalyst. In comparison, the formation of 2-propoxide after 2-propanol adsorbed on TiO_2 powder makes 2-propanol oxidation much faster than on TiO_2/PVG. It may be possible in the future to combine such catalytic surfaces to ensure the efficient PCO of 2-propanol and acetone.

ACKNOWLEDGMENTS

The authors thank Joseph Francisco for the use of the FTIR instrument and Sarah Pilkenton for a careful reading of the manuscript. This work was

supported by the NSF (CHE-97-33188, CAREER grant) and the donors of Petroleum Research Fund, administered by the American Chemical Society. W.X. thanks Purdue's Environmental Science and Engineering Institute for a graduate fellowship. D.R. is an A.P. Sloan Foundation Fellow (1999–2001).

REFERENCES

1. Alberici, R. M., and Jardim, W. F., *Appl. Catal. B Environ.* **14**, 55 (1997).
2. Fox, M. A., and Dulay, M. T., *Chem. Rev.* **93**, 341 (1993).
3. Hoffmann, M. R., Martin, S. T., Choi, W., and Bahnemann, D. W., *Chem. Rev.* **95**, 69 (1995).
4. Linsebigler, A. L., Lu, G. Q., and Yates, J. T., *Chem. Rev.* **95**, 735 (1995).
5. Peral, J., and Ollis, D., *J. Catal.* **136**, 554 (1992).
6. Vorontsov, A. V., Barannik, G. B., Snegurenko, O. I., Savinov, E. N., and Parmon, V. N., *Kinet. Catal.* **38**, 84 (1997).
7. Stevens, L., Lanning, J. A., Anderson, L. G., Jacoby, W. A., and Chornet, N., *J. Air Waste Manag. Assoc.* **48**, 979 (1998).
8. Hager, S., and Bauer, R., *Chemosphere* **38**, 1549 (1999).
9. Munuera, G., and Stone, F. S., *Faraday Discuss. Chem. Soc.* **52**, 205 (1971).
10. Larson, S. A., Widegren, J. A., and Falconer, J. L., *J. Catal.* **157**, 611 (1995).
11. Chen, S., Cheng, X., Tao, Y., and Zhao, M., *J. Chem. Technol. Biotechnol.* **73**, 264 (1998).
12. Bickley, R. I., Munuera, G., and Stone, F. S., *J. Catal.* **31**, 398 (1973).
13. Bickley, R. I., and Jayanty, R. K. M., *Faraday Discuss. Chem. Soc.* **58**, 194 (1974).
14. El-Maazawi, M., Finken, A. N., Nair, A. B., and Grassian, V. H., *J. Catal.* **191**, 138 (2000).
15. Xu, W., and Raftery, D., *J. Phys. Chem. B* **105**, 4343 (2001).
16. Hwang, S.-J., Petucci, C., and Raftery, D., *J. Am. Chem. Soc.* **119**, 7877 (1997).
17. Hwang, S.-J., Petucci, C., and Raftery, D., *J. Am. Chem. Soc.* **120**, 4388 (1998).
18. Rice, C. V., and Raftery, D., *Chem. Commun.* 1 (1999).
19. Hwang, S.-J., and Raftery, D., *Catal. Today* **1579**, 1 (1999).
20. Pilkenton, S., Hwang, S.-J., and Raftery, D., *J. Phys. Chem. B* **103**, 11,152 (2000).
21. Pilkenton, S., Xu, W., and Raftery, D., *Anal. Sci.* **17**, 25 (2001).
22. Xiang, Y., Larsen, S. C., and Grassian, V. H., *J. Am. Chem. Soc.* **121**, 5063 (1999).
23. Panov, A. G., Larsen, R. G., Totah, N. I., Larsen, S. C., and Grassian, V. H., *J. Phys. Chem. B* **104**, 5706 (2000).
24. Raupp, G. B., and Junio, C. T., *Appl. Surf. Sci.* **72**, 321 (1993).
25. Sauer, M. L., and Ollis, D. F., *J. Catal.* **149**, 81 (1994).
26. Nimlos, M. R., Jacoby, W. A., Blake, D. M., and Mline, T. A., *Environ. Sci. Technol.* **27**, 732 (1993).
27. Matsubara, H., Takada, M., Koyama, S., Hashimoto, K., and Fujishima, A., *Chem. Lett.* 767 (1995).
28. Wong, J. C. S., Linsebigler, A., Lu, G. Q., Fan, J. F., and Yates, J. T., *J. Phys. Chem.* **99**, 335 (1995).
29. Fan, J. F., and Yates, J. T., *J. Am. Chem. Soc.* **118**, 4686 (1996).
30. Driessen, M. D., Goodman, A. L., Miller, T. M., Zaharias, G. A., and Grassian, V. H., *J. Phys. Chem. B* **102**, 549 (1998).
31. Miller, M. L., Borisch, J., Raftery, D., and Francisco, J. S., *J. Am. Chem. Soc.* **120**, 8265 (1998).
32. Anpo, M., Aikawa, N., and Kubokawa, Y., *J. Phys. Chem.* **89**, 5017 (1985).
33. Anpo, M., Sunamoto, M., and Che, M., *J. Phys. Chem.* **93**, 1187 (1989).
34. Yamashita, H., Ichihashi, Y., Harada, M., Steward, G., Fox, M. A., and Anpo, M., *J. Catal.* **158**, 97 (1996).
35. Kawamura, H., Okuto, S., Taruta, S., Takusagawa, N., and Kitajima, K., *J. Ceram. Soc. Jpn.* **104**, 1160 (1996).
36. Yamashita, H., Honda, M., Harada, M., Ichihashi, Y., and Anpo, M., *J. Phys. Chem. B* **102**, 10,707 (1998).
37. Yu, J., Lin, J., and Kwok, R. W. M., *J. Photochem. Photobiol., A Chem.* **111**, 199 (1997).
38. Anpo, M., and Chiba, K., *J. Mol. Catal.* **74**, 207 (1992).
39. Xu, T., Munson, E. J., and Haw, J. F., *J. Am. Chem. Soc.* **116**, 1962 (1994).
40. Zaki, M. I., Hasan, M. A., Al-Sagheer, F. A., and Pasupulety, L., *Langmuir* **16**, 430 (2000).
41. "Sadtler Standard Carbon-13 NMR Spectra." Bio-Rad Laboratories, Philadelphia, PA, 1994.
42. Root, T. W., and Duncan, T. M., *J. Catal.* **101**, 527 (1986).
43. Root, T. W., and Duncan, T. M., *J. Catal.* **102**, 109 (1986).
44. Xu, W., Raftery, D., and Francisco, J., in preparation.
45. Biaglow, A. I., Gorte, R. J., Kokotailo, G. T., and White, D., *J. Catal.* **148**, 779 (1994).
46. Barich, D. H., Nicholas, J. B., Xu, T., and Haw, J. F., *J. Am. Chem. Soc.* **120**, 12,342 (1998).
47. Galan-Fereres, M., Alemany, L. J., Mariscal, R., Banares, M. A., Anderson, J. A., and Fierro, J. L. G., *Chem. Mater.* **7**, 1342 (1995).